FC-PAD

Fuel Cell – Performance and Durability

FC136 – Electrocatalysts and Supports

Thrust Coordinator: Debbie Myers

June 8, 2016

This presentation does not contain any proprietary, confidential, or otherwise restricted information.

Component Thrust 1: Electrocatalysts and Supports

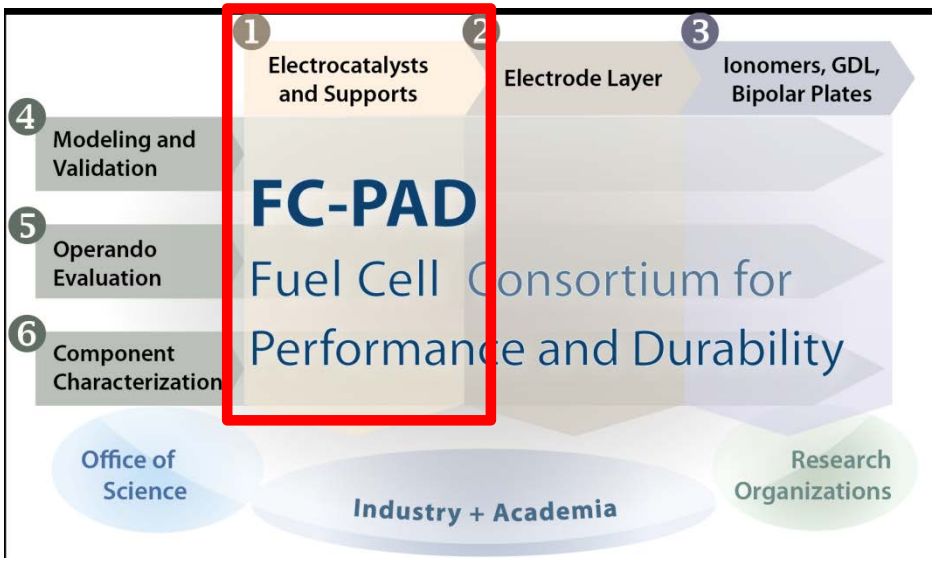

Overview:

- Three component thrusts focusing on catalyst, electrode and ionomer/GDL/plates
- Three crosscutting thrusts focusing on modeling, evaluation, and characterization

- Thrust Area 1, Electrocatalysts and Supports, is the focus of this presentation
- Thrust Area 1 is synergistic with Thrust Areas 2, 3, and 5 and supported by Thrust Areas 4 and 6

FC-PAD contributors to this presentation

Argonne NATIONAL LABORATORY

Debbie Myers
Nancy Kariuki
Xiaoping Wang
Dennis Papadias
Rajesh Ahluwalia

Los Alamos NATIONAL LABORATORY

Rangachary Mukundan
Rod Borup
Yu Seung Kim

NREL NATIONAL RENEWABLE ENERGY LABORATORY

Shyam Kocha
KC Neyerlin
Jason Christ
Jason Zack

OAK RIDGE National Laboratory

Karren More
David Cullen

Current Collaborators

- IRD (Catalysts, MEAs)
- Umicore (Catalysts)
- Johnson Matthey (Catalysts, CCMs; as part of FC106)
- Ion Power (CCMs)
- Korea Institute of Energy Research (micro-electrode cell studies)

FC-PAD Thrust 1: Overview

Timeline

- Project start date: 10/01/2015
- Project end date: 09/30/2020

National Labs

- ANL, LANL, NREL, and ORNL

Partners/Collaborators To Date

- IRD, New Mexico
- Umicore, Germany
- NECC, Japan
- GM, USA
- Ion Power, USA
- Tanaka Kikinzoku Kogyo (TKK), Japan
- Johnson Matthey, United Kingdom
- Korea Institute of Energy Research (KIER)
- Partners to be added by DOE DE-FOA-0001412

Barriers

- The electrocatalyst remains a challenge for reducing the **cost** to meet system cost targets

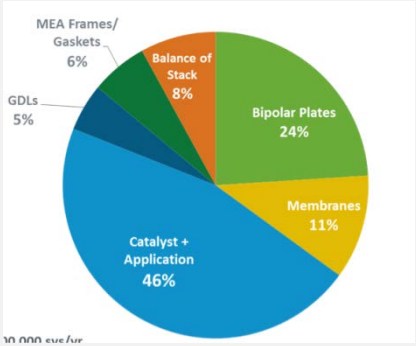

- **Durability** targets have not been met
- The **catalyst, its interaction with other electrode components, the stability of alloying components, and the effect of this instability are** not fully understood and are key to achieving performance, cost, and durability targets.

FUEL CELL PERFORMANCE AND DURABILITY

Relevance and Approach

- **Thrust Area Objectives**
  - Realize the ORR mass activity benefits of advanced Pt-based cathode electrocatalysts in high current density, air performance for over 5,000 operating hours and with low PGM loading (<0.1 mg-Pt/cm^2)

Approach - Achieve Objectives by studying:

- **Catalyst and catalyst support durability and degradation mechanisms**
  - *Elucidate catalyst and support degradation mechanisms as a function of catalyst and support physicochemical properties and cell operating conditions*
  - *Quantify catalyst and support stability during accelerated stress tests and start-up and shut-down transients using in-cell measurements*
  - *Determine stability of catalyst components, catalyst and support composition and structural changes*
- **Catalyst/support interactions**
  - Understand interplay between the catalyst and support properties and their mutual interactions
  - *Determine the effects of carbon type (e.g., high, medium, and low surface area) and carbon dopants on the strength of the catalyst/support and ionomer/support interactions*
  - Investigate the impact of these interactions on catalyst and support stability, durability, and performance
- **Ex-situ analysis of catalyst instability on cathode-catalyst-layer properties**
  - *Quantify the impact of catalyst degradation on the properties defining the performance of the cathode catalyst layer (e.g., impact of base metal leaching from Pt alloy catalyst on proton conductivity, oxygen permeability, and water uptake in ionomer)*

Electrocatalysts currently under study in FC-PAD

Commercial Sources

- **IRD:**
  - IRD CAT0023, 55wt% PtCo/C, 6.0 nm TEM ✓
- **Umicore:**
  - Elyst Pt50 0550; 45.9wt% Pt, 5.5 nm XRD ✓
  - Elyst P30 0670; 27.5 wt% Pt; 3 wt% Co, 4.4 nm TEM ✓
- **NEChemcat:**
  - PtCo/NE-GM ✓
  - Core-shell Pt ML/Pd/NE-H ✓
- **TKK:**
  - TEC10E50E, Pt/HSC, 47.5wt% Pt, 2.5 nm XRD ✓
  - TEC36E52, Pt_3Co/HSC, 46.5 wt% Pt, 4.7 wt% Co, 5.7 nm TEM ✓
- **Johnson Matthey:**
  - Pt_3Co/HSC, 40 wt% Pt, 4.9, 8.7, 14.3 nm TEM ✓
  - Dealloyed-$Pt_{1.3}Ni$/HSC, 29.1 wt% Pt, 6.68 wt% Ni, 5.1 nm TEM ✓

National Lab Sources

- NREL ETFECS ✓
- ANL Frame ✓

Automotive

- General Motors
  - Proprietary ✓

Academic

- USC Pt/ACCC ✓

Electrocatalysts being studied for foundational understanding of advanced catalysts

Platinum Alloy Electrocatalysts in FC-PAD

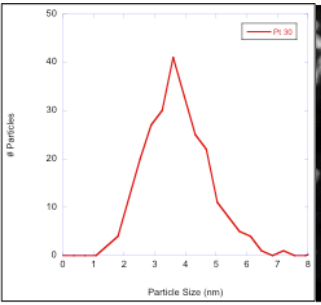

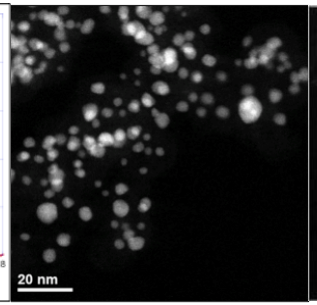

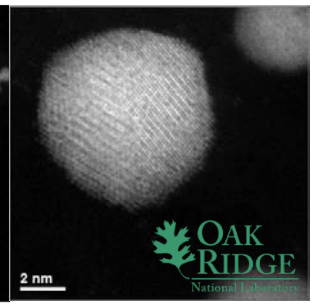

Umicore Pt_7Co_3/C
Mean particle size of 4.4 nm

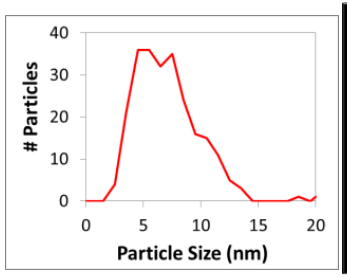

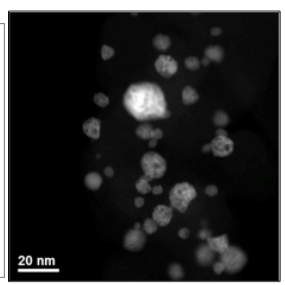

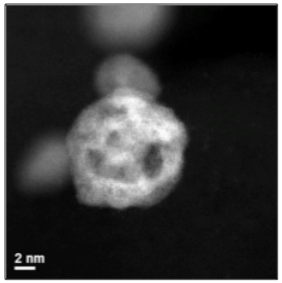

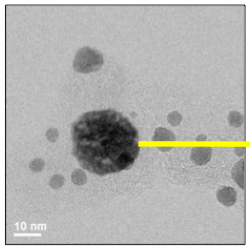

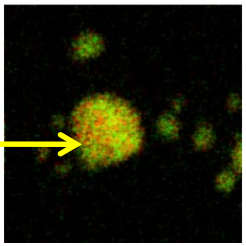

"Spongy" PtCo morphology

OAK RIDGE National Laboratory

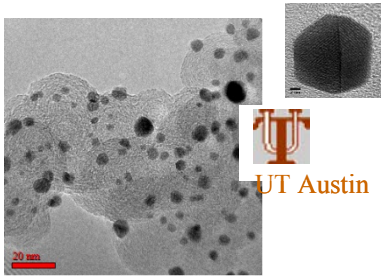

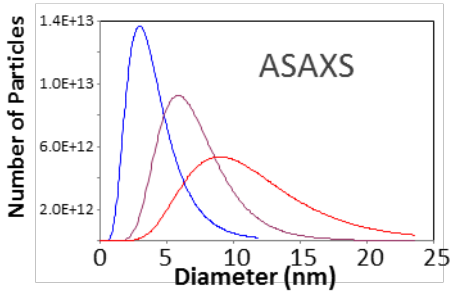

IRD PtCo/C
Mean particle size of 6.0 nm

Three JM Pt_3Co/C
Mean particle sizes of
4.9, 8.7, 14.3 nm

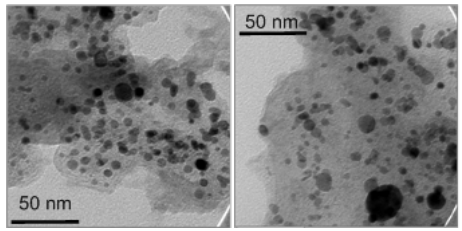

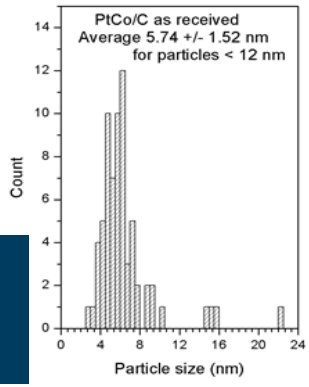

TKK Pt_3Co/C
Mean particle size of 5.7 nm

FCPAD
FUEL CELL PERFORMANCE AND DURABILITY

Accomplishment: *Ex situ* measurement of ORR Activity

NREL
NATIONAL RENEWABLE ENERGY LABORATORY

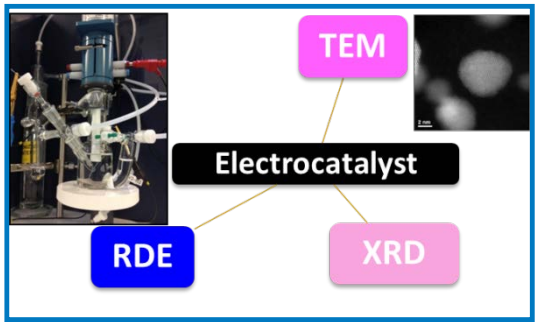

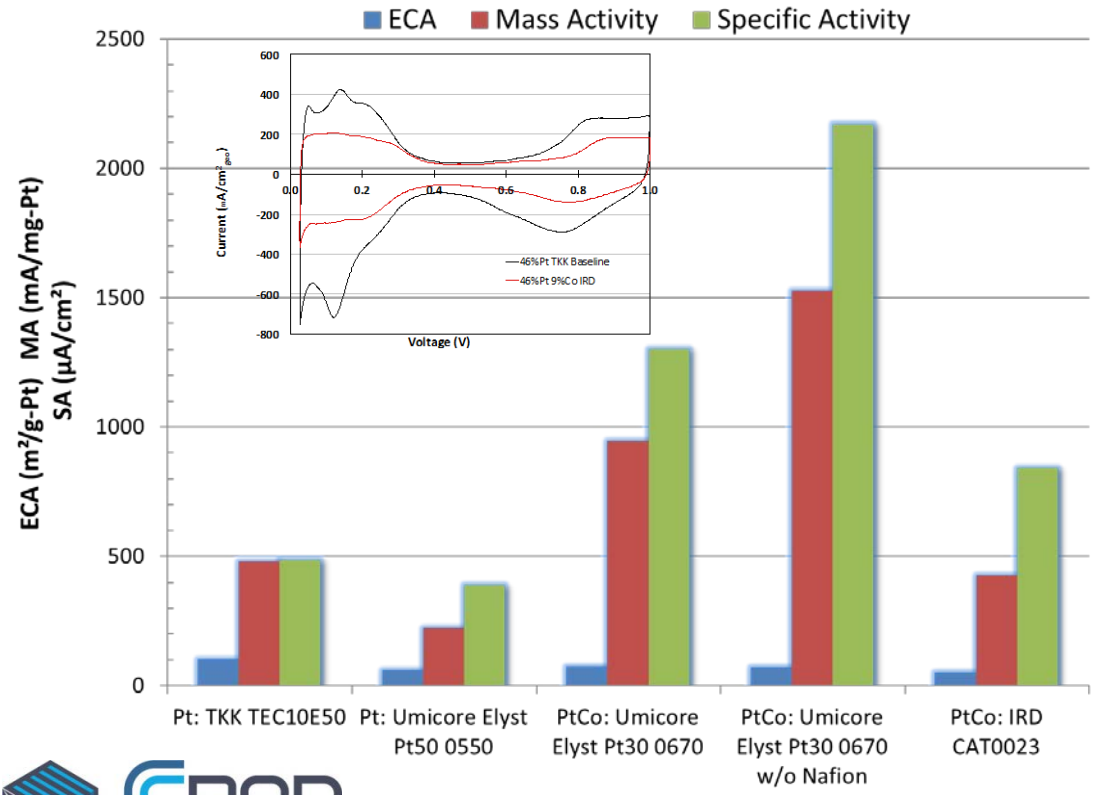

- Baseline oxygen reduction reaction (ORR) activity of catalysts determined using thin-film rotating disk electrode (RDE) method developed and described in FC111 (with ionomer in thin film)
- Electrochemically-active surface area of "baseline" high surface area Pt (TKK TEC10E50) is twice that of platinum alloy catalysts due to alloying heat treatment step leading to particle growth
- Ionomer in electrode suppresses ORR activity, by 40% for Umicore Pt_3Co
- IRD PtCo catalyst showed lower ORR activity in RDE than in MEA (cf. FC137)
- **Platinum alloys under consideration meet or exceed DOE 2020 ORR activity target (>440 mA/mg-Pt)**

FCPAD
FUEL CELL PERFORMANCE AND DURABILITY

Accomplishment: Potential Dependence of Pt and Co dissolution

ICP-MS detection of dissolved metals in 0.57 M $HClO_4$

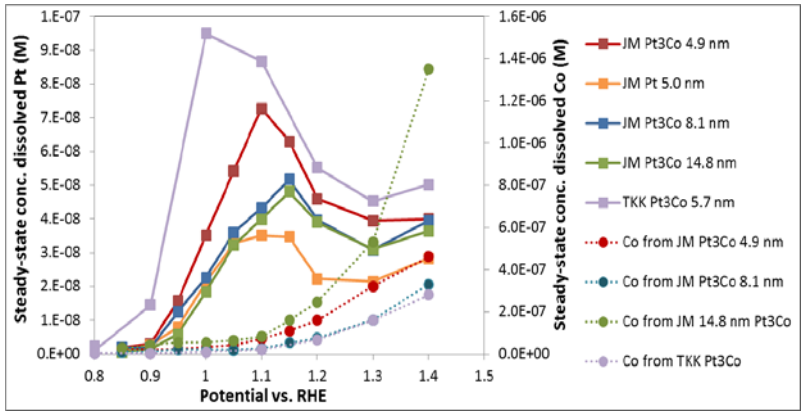

Solid Squares: TKK 5.7 nm Pt_3Co potentiostatic
Solid diamonds: TKK 5.7 nm Pt3Co potential cycling
Open Diamonds: IRD 7.2 nm Pt_3Co Cycling

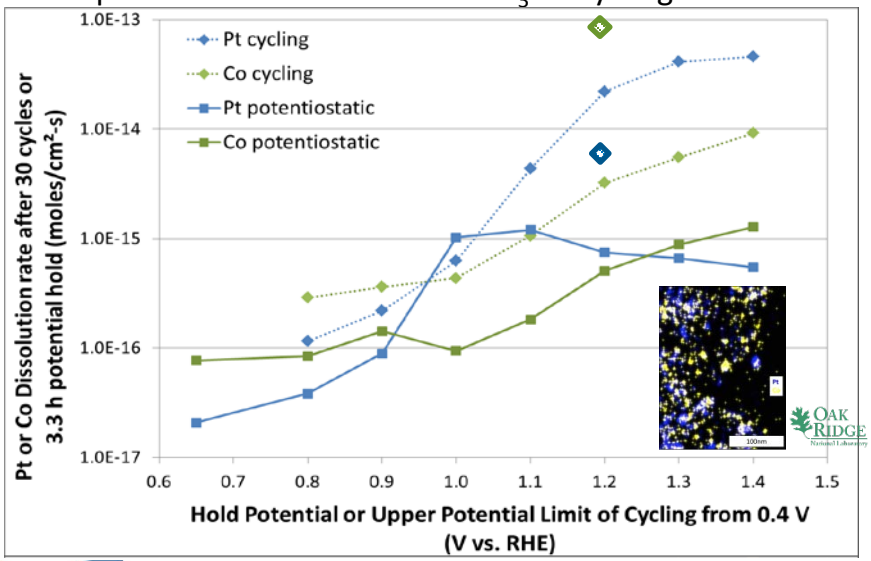

- Potentiostatic Pt dissolution increases with decreasing particle size for the JM Pt_3Co catalysts
- Potentiostatic Co dissolution is highest for the JM Pt_3Co/C catalyst with the largest particle size
- TKK 5.7 nm Pt_3Co catalyst shows a higher extent of Pt dissolution than all of the JM catalysts, even those with much larger particle size
- Pt dissolution is higher for JM 4.9 nm Pt_3Co as compared to that of a Pt catalyst with very similar PSD (5.0 nm Pt)
- Steady-state Co dissolution increases with increasing potential above 1.1 V, consistent with potentiostatic and potential cycling dissolution rate data
- Potential cycling Pt dissolution rate lower for IRD "spongy" Pt_3Co compared to TKK "solid" Pt_3Co, whereas **Co dissolution rate is much higher**
- Dissolution data illustrate detrimental impact of cell voltages >1.0 V on base metal retention in nanoparticles

Accomplishment: Potential Dependence of Alloy Catalyst Oxidation

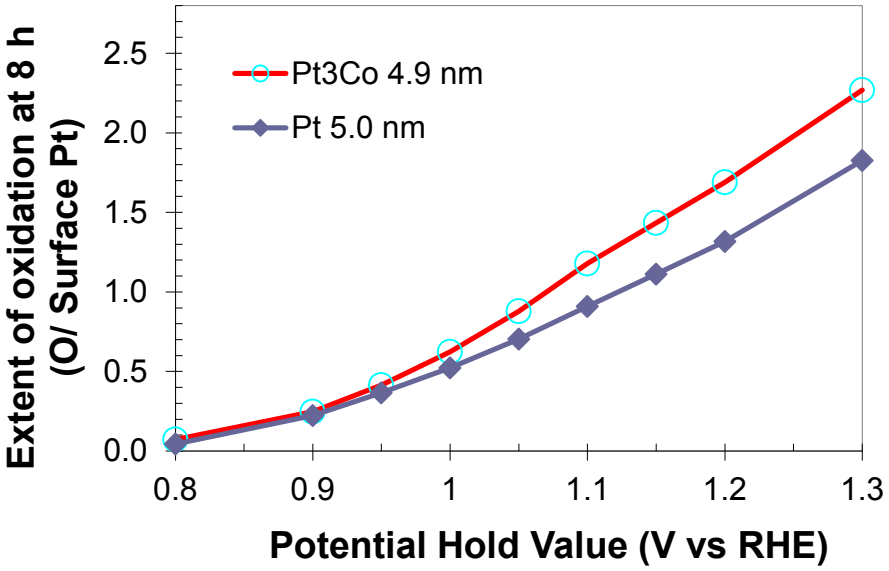

- Extent of Oxidation determined via voltammetric charge for oxide reduction after 8 hour potential holds in dilute aqueous $HClO_4$ electrolyte

- Extent of oxidation determined via height of Pt L_3 X-ray absorption "white line" after 30 min potential holds in dilute aqueous $HClO_4$ electrolyte

- Pt alloy particles show greater extent of oxidation of surface Pt than Pt particles having approximately the same size distribution.

- These data, and cyclic voltammetry data, are used as input to the dissolution model to find the links between oxide formation and dissolution under potentiostatic and potential cycling conditions.

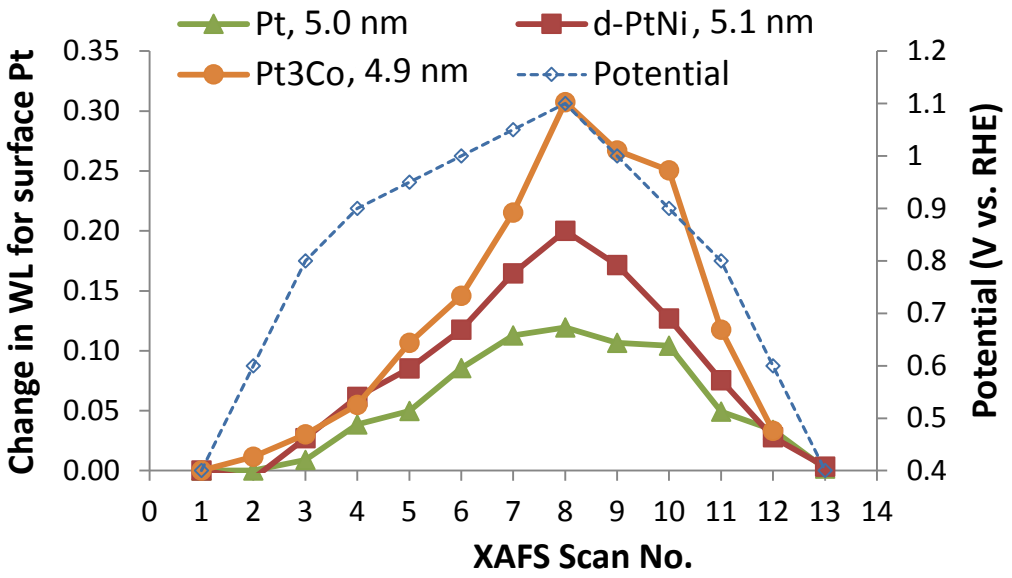

FUEL CELL PERFORMANCE AND DURABILITY

Accomplishment: Thermodynamics of PtO_x Formation Pt_3Co Alloy

Solid solution model for PtO_x formation

- $Pt + H_2O = PtOH + H^+ + e^-$
- $PtOH = PtO + H^+ + e^-$
- $PtO + H_2O = PtO_2 + 2H^+ + 2e^-$

XPS Study and DFT/Monte Carlo Simulations*

- Potentials < 0.65 V, $H_2O_{(ad)}$ is the dominant species
- Above 0.65 V, $OH_{(ad)}$ forms from oxidation of $H_2O_{(ad)}$
- Above 0.8 V, $OH_{(ad)}$ further oxidizes to $O_{(ad)}$

Oxidation of Pt in Pt_3Co to PtO_x is only weakly dependent on particle size

- PtO_x estimated from the CV reduction charge (Q) after 8-h hold at potential
- Developed a sequential procedure for determining the activities of Pt, PtOH, PtO and PtO_2 in the mixed surface oxide solution

$$K_i = c_{H^+}\left(\frac{\theta_i}{\theta_{i-1}}\right)e^{-\frac{nF}{RT}[E-E_{0i}]} = a_i e^{-\frac{\omega_i}{RT}\theta_i^{x_i}}$$

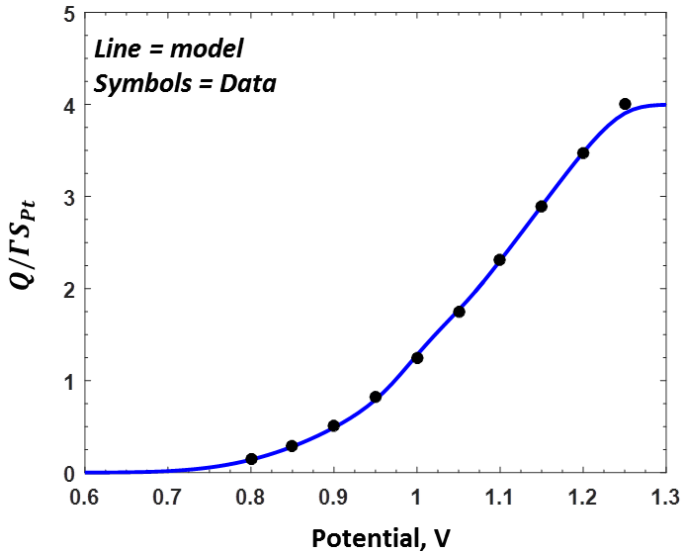

All data from aqueous tests with 0.57 M $HClO_4$

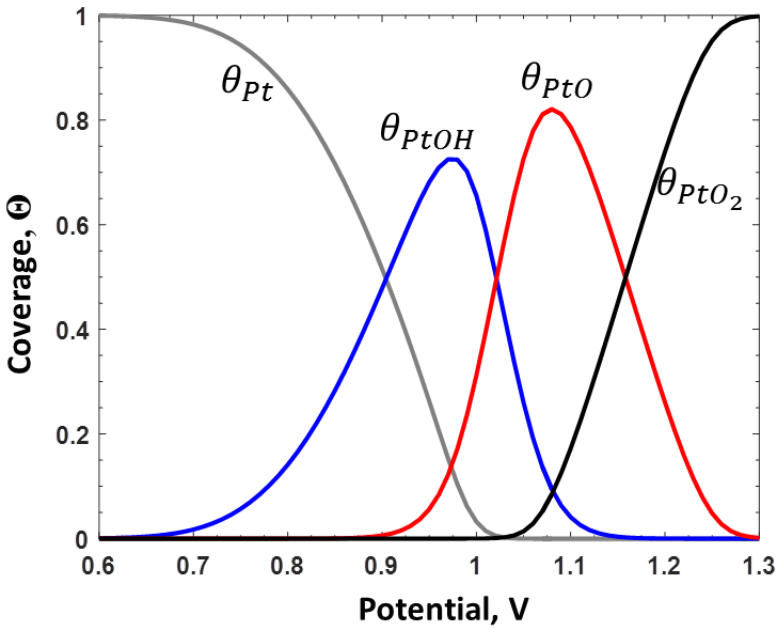

H.S. Casalongue, et al., "Direct observation of the oxygenated species during oxygen reduction reaction on a platinum fuel cell cathode", Nature Communications, Dec, 2013.

FUEL CELL PERFORMANCE AND DURABILITY

Accomplishment: Kinetics of PtO_x Formation for Pt_3Co Alloy

Developed a procedure for determining the rate constants for kinetics of PtO_x formation by using the CV oxidation and reduction scans (8 h hold at high potential, 10 mV/s scan rate)

- **Only 10-30 s needed to form or reduce the oxides during the potential scans**

	Oxidation Potential (E_0)	Symmetry Factor (α)
$Pt + H_2O = PtOH + H^+ + e^-$	0.740 V	0.735
$PtOH = PtO + H^+ + e^-$	1.220 V	0.6
$PtO + H_2O = PtO_2 + 2H^+ + 2e^-$	1.045 V	0.55

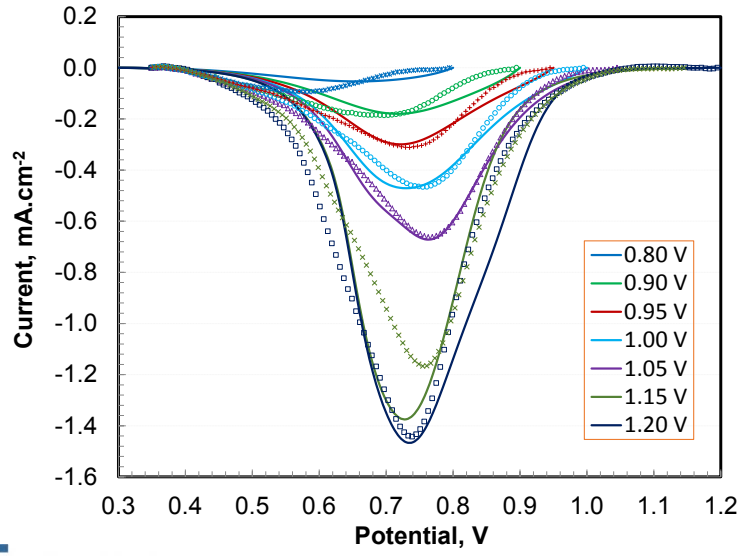

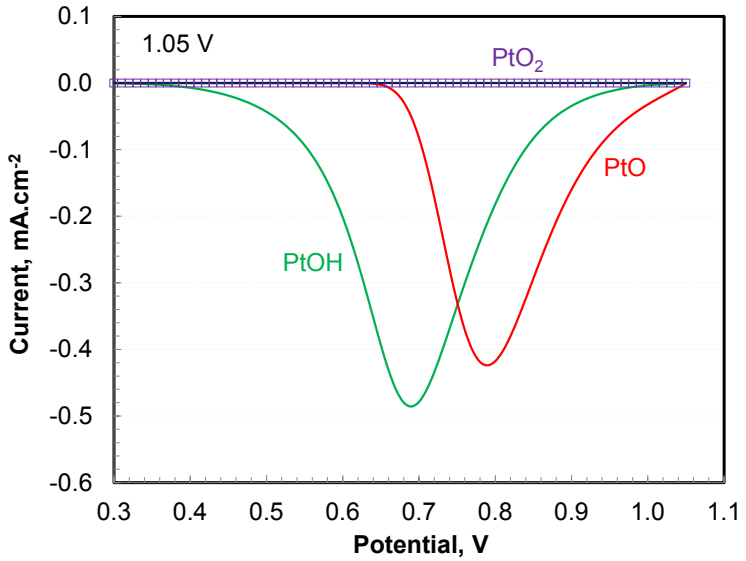

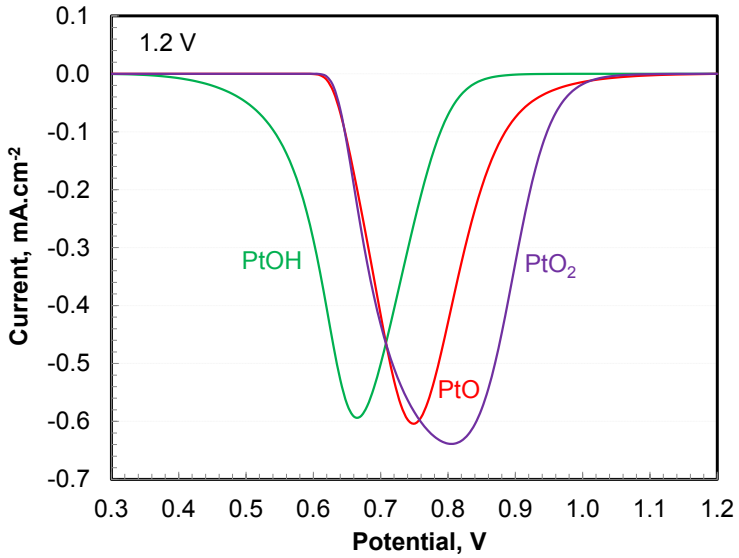

FUEL CELL PERFORMANCE AND DURABILITY

Accomplishment: Thermodynamics of Pt dissolution from Pt_3Co Alloy

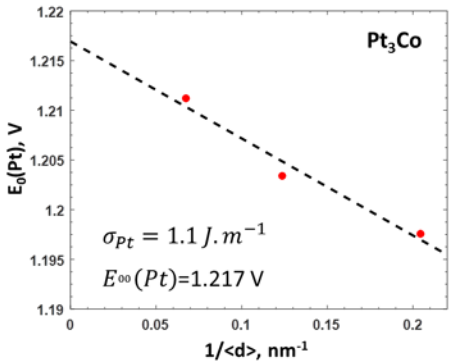

Standard potential (E_0) for Pt dissolution ($Pt = Pt^{2+} + 2e^-$) from Pt_3Co alloy and its dependence on particle diameter

- **Pt_3Co has higher E_0 than Pt** and is more stable at low potentials

Derived from dissolution data at 0.85 V

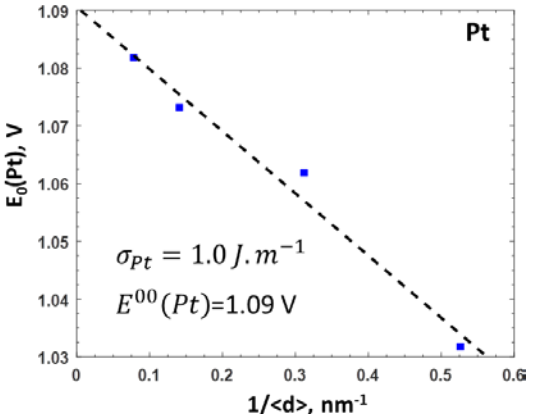

Thermodynamics of electrochemical and chemical dissolution of Pt

- $Pt = Pt^{2+} + 2e^-$
- $PtOH + H^+ = Pt^{2+} + H_2O + e^-$
- $PtO + 2H^+ = Pt^{2+} + H_2O$
- $PtO_2 + 4H^+ + 2e^- = Pt^{2+} + 2H_2O$

Equilibrium Constants

- Electrochemical dissolution

$$K_i = \left(\frac{C_{Pt^{2+}}}{\theta_i}\right) e^{-\frac{nF}{RT}[E - E_{0i}]}$$

- Chemical dissolution

$$K_{PtO} = \left(\frac{C_{Pt^{2+}}}{\theta_{PtO}}\right) \frac{1}{c_{H^+}^2}$$

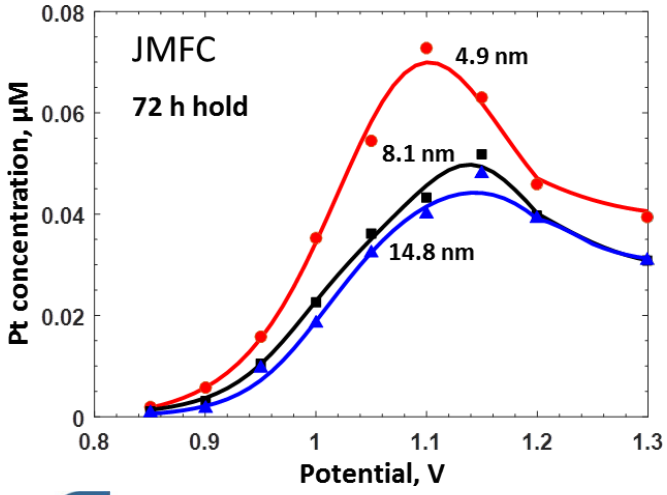

Pt_3Co has higher dissolution potential, but is less stable than Pt at high potentials

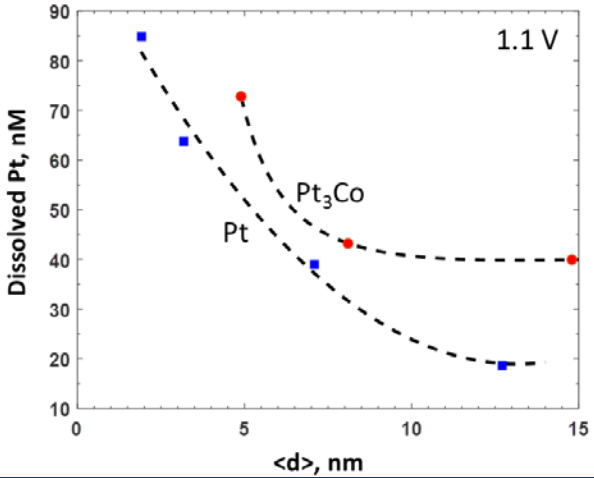

Accomplishment: Kinetics of Pt dissolution from Pt_3Co Alloy

Rate constants derived from potentiostatic dissolution predict the behavior observed in cyclic tests: triangle wave, 10 mV/s scan rate, fixed lower potential limit (0.4 V), variable upper potential limit

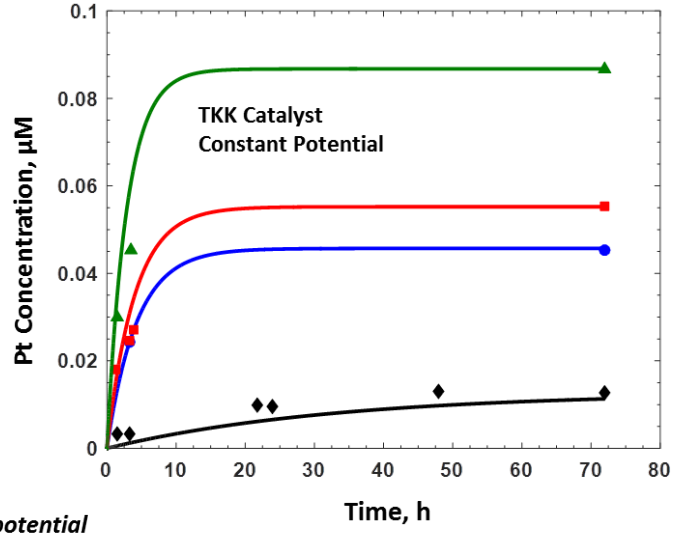

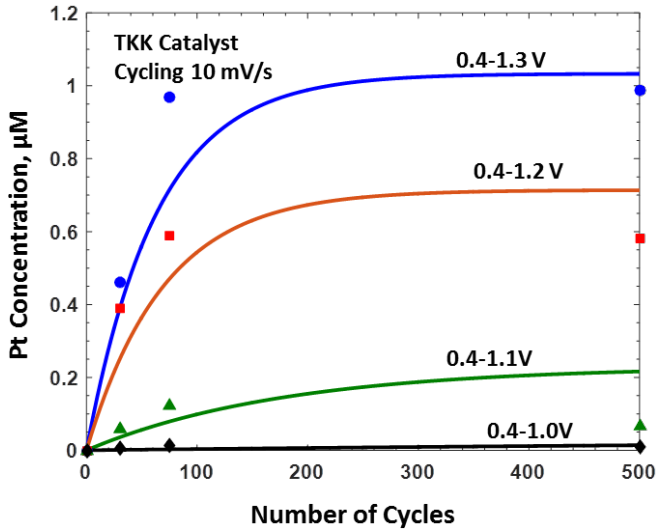

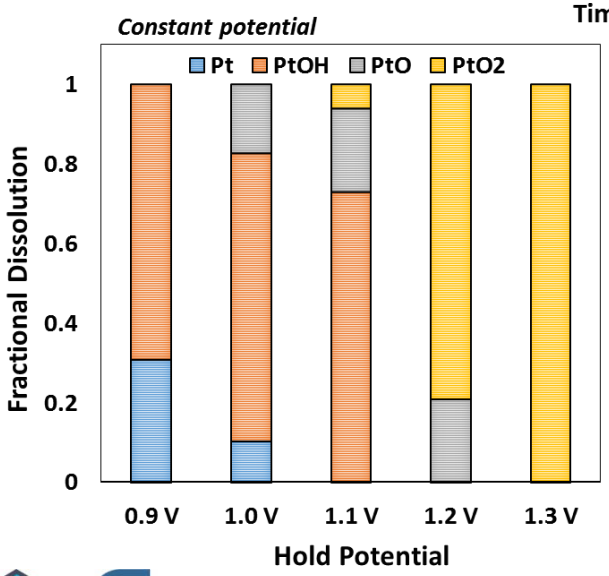

Cyclic Potential Dissolution

Upper Potential Limit Above 1.1 V

- Pt dissolves as PtOH
- Pt^{2+} re-deposits as Pt during cathodic scan

Upper Potential Limit Below 1.1 V

- Pt dissolves as Pt and PtOH
- No significant re-deposition during cathodic scan

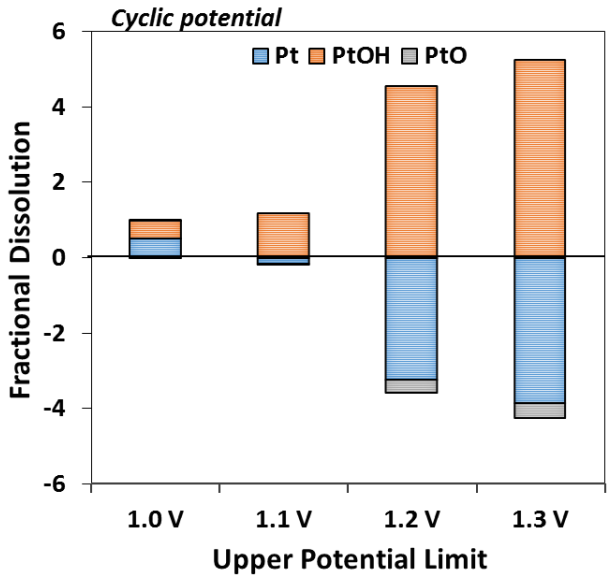

FUEL CELL PERFORMANCE AND DURABILITY

Accomplishment: Thermodynamics of Co Dissolution from Pt_3Co Alloy

Surface Co is thermodynamically unstable (E_0=0.280 V) and dissolves during pre-treatment to create a core-shell structure. The thickness of Pt skin is proportional to particle size.

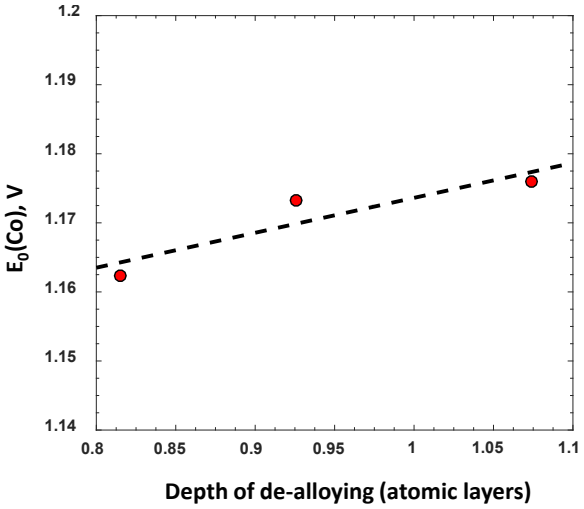

Sub-surface Co (SS-Co) has a dissolution potential (E_0) of 1.158 V, and it increases as Pt skin gets thicker.

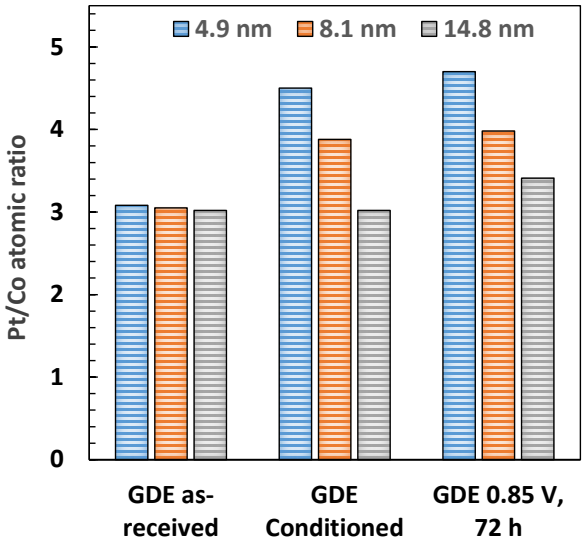

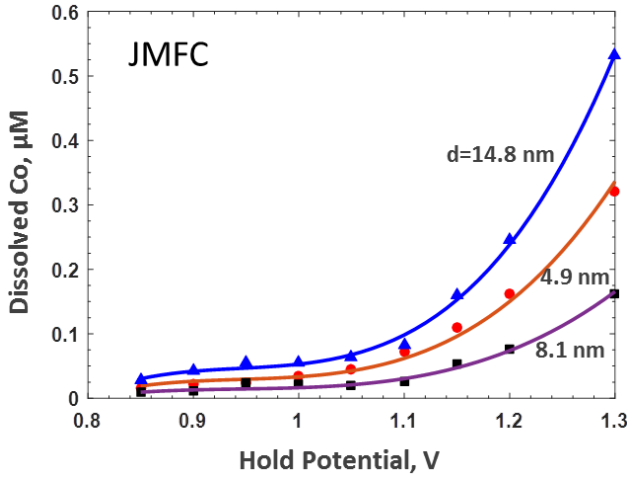

At higher potentials, SS-Co may be stabilized by the formation of sub-surface oxides of Co.

- Oxygen can coordinate with SS-Co: ΔG = -166 kJ/mol for PtO + Co = Pt + CoO
- XANES measurements of $\Delta\mu$ for dealloyed PtM_3

$$lna_{Co} = lnc_{Co^{2+}} - (E - E_0)\frac{2F}{RT}$$

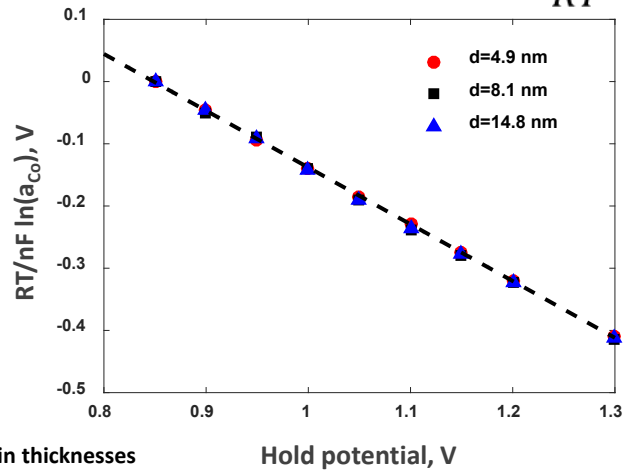

KM Caldwell, et al., "Spectroscopic in situ measurements of the relative Pt skin thicknesses and porosities of dealloyed PtM_n (Ni, CO) electrocatalysts", Phys. Chem. C, 757-765, 2015.

FUEL CELL PERFORMANCE AND DURABILITY

Accomplishment: Kinetics of Co Dissolution from Pt_3Co Alloy

The rate constant for SS-Co dissolution depends on potential/surface oxides

- Need fundamental understanding of oxygen coordination with Co in core-shell Pt_3Co

Under potential cycling, the kinetics of change in SS-Co activity are slow

- The derived activity on a repeat cycle is far from equilibrium and shows hysteresis
- 10-50 times higher Co dissolution after 500 triangle cycles (17-25 h) than potentiostatic hold for 72 h
- Difficult to correlate the changes in activities of SS-Co and Pt oxides in Pt_3Co

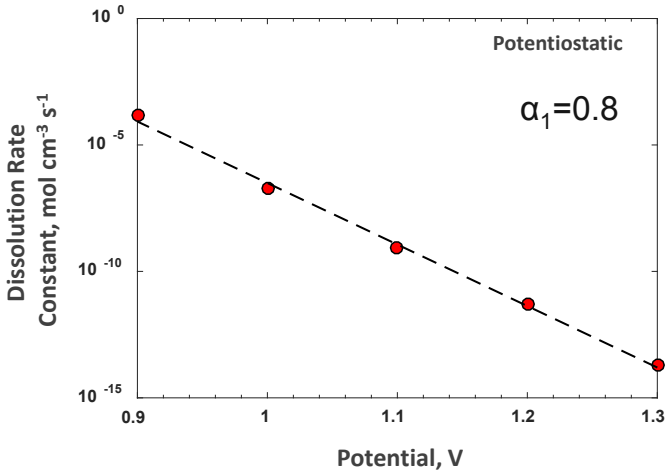

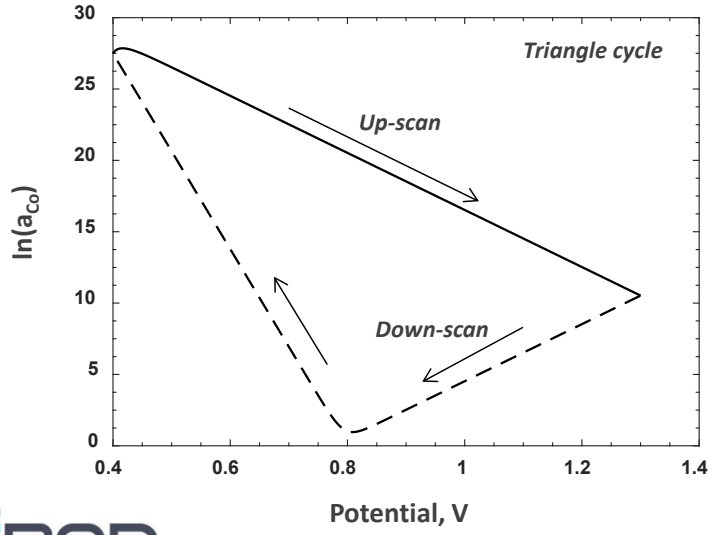

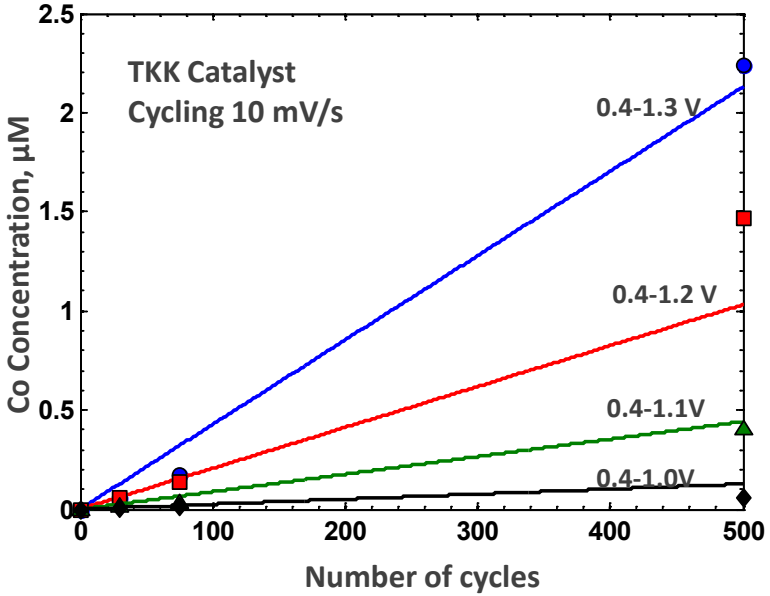

Impact of Base Metal on Ionomer Oxygen Permeability

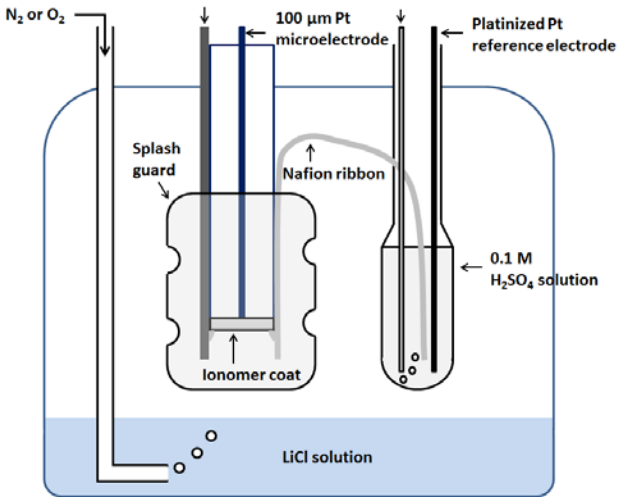

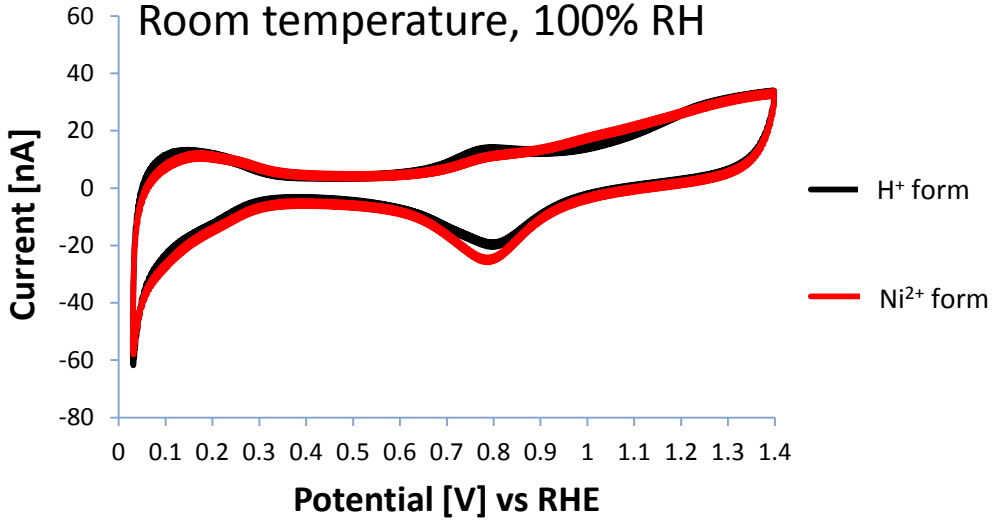

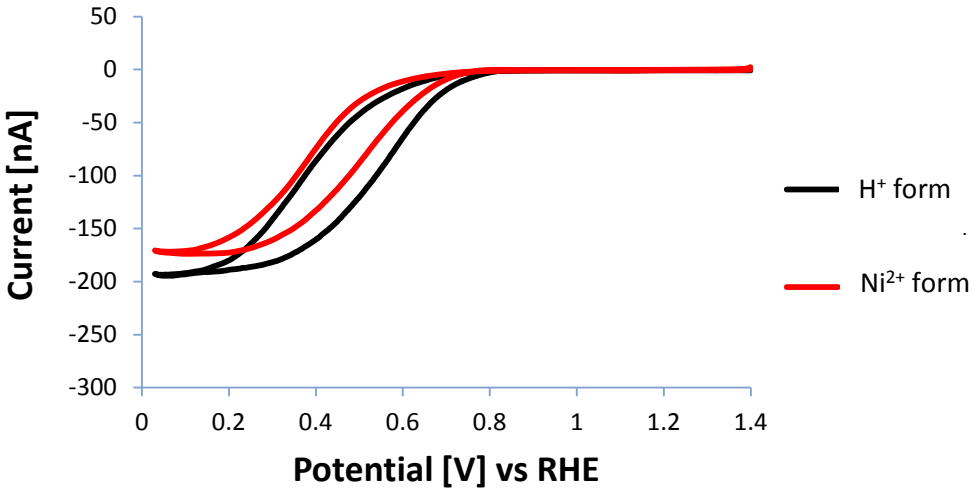

- RDE showed 6% decrease in oxygen permeability of 0.7 µm ionomer film for 10 mM Ni^{2+} in 0.1 M $HClO_4$; 29% decrease in ORR kinetic current at 0.9 V. (FC106; 2015 AMR)
- Solid state microelectrode cell showed ~15% decrease in oxygen permeability with addition of $Ni(ClO_4)_2$ and decrease in ORR kinetics

FUEL CELL PERFORMANCE AND DURABILITY

Los Alamos NATIONAL LABORATORY

KIER ENERGY TECHNOLOGIES

Carbon Corrosion Measurement Matrix for Mechanistic Definition

Carbon thermodynamics

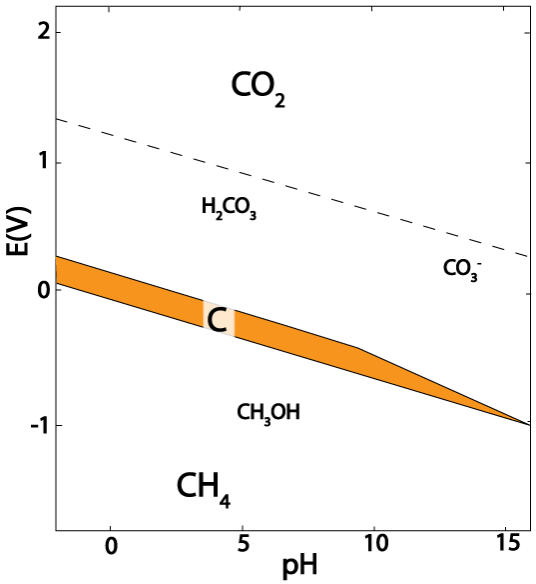

Adapted from M. Pourbaix, *Atlas of Electrochemical Equilibria* (1966)

- Experimentally measure carbon corrosion during operation
  - Direct CO_2 measurement by NDIR
- Modeling to identify carbon corrosion mechanism and rates related to carbon and Pt surface oxidation

Three Types of Carbon Supports

E (High Surface Area, Ketjen); TEC10E20E; 18.5 wt% Pt/C, 0.15 mg-Pt/cm²
EA (Graphitized or Low Surface Area); TEC10EA40E, 38.7 wt% Pt/C, 0.25 mg-Pt/cm²
V (Vulcan); TEC10V40E, 33.9 wt% Pt, 0.17 mg-Pt/cm²

Ion Power MEAs with SGL 25BC GDLs in 50-cm² quad-serpentine flow field from Fuel Cell Technologies, 80°C cell temp.; H2: 670 sccm, 83°C dew point, 3.4 psig; Air: 1800 sccm, 83°C dew point

Vary Upper Potential Limit
0.95 V – 0.40 V
0.90 V – 0.40 V
0.85 V – 0.40 V
…..
0.55 V – 0.40 V

Vary Lower Potential Limit
0.95 V – 0.40 V
0.95 V – 0.45 V
0.95 V – 0.50 V
…..
0.95 V – 0.80 V

Potential Reset Times
0.5 min
1 min
2 min
5 min

Fuel Cell operation largely as per DOE/FCTT Drive Cycle Protocol

Measured Carbon Corrosion During Drive-Cycle

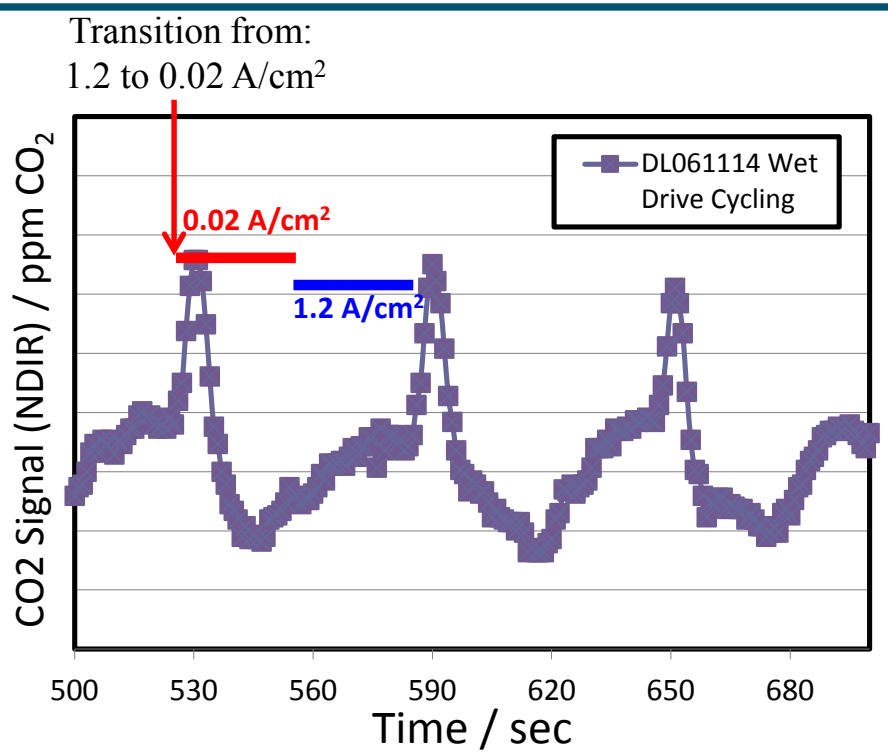

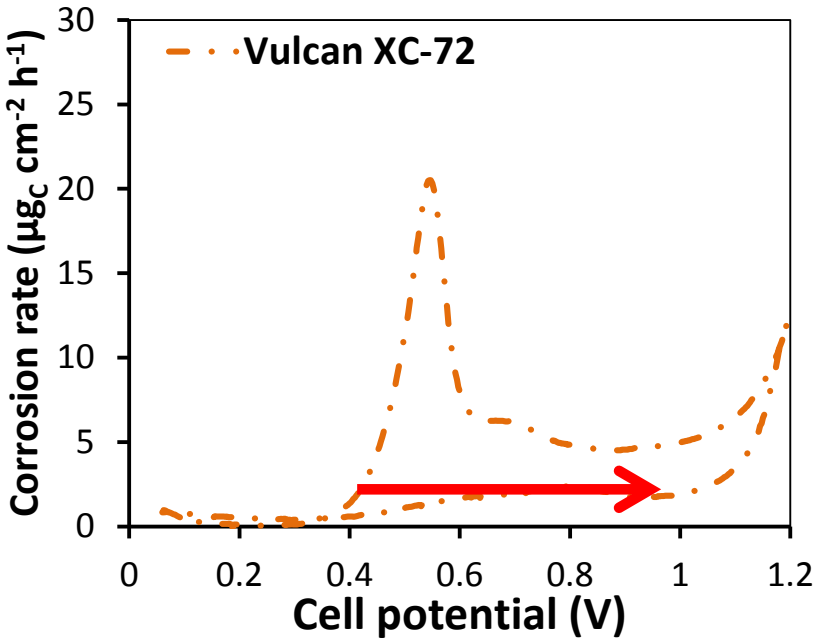

- Non-zero CO_2 evolution with all carbon types during drive cycle
- As power decreases, voltage increases
- During voltage rises, CO_2 evolves from the catalyst
- After spike, CO_2 evolution is reduced
  - surface passivation
- Higher 'steady-state' CO_2 production at 1.2 A/cm²
  - reducing surface/forming adsorbed species

Los Alamos

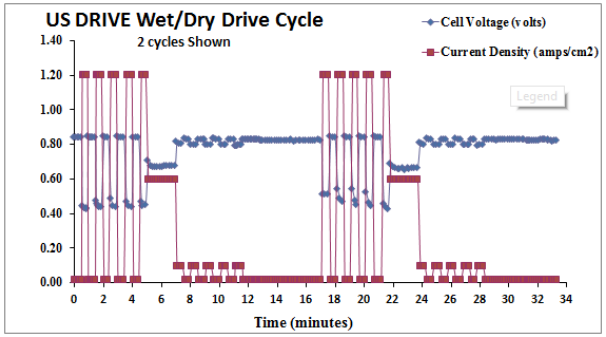

FCPAD FUEL CELL PERFORMANCE AND DURABILITY

Accomplishment: Comparison of corrosion of three carbon types

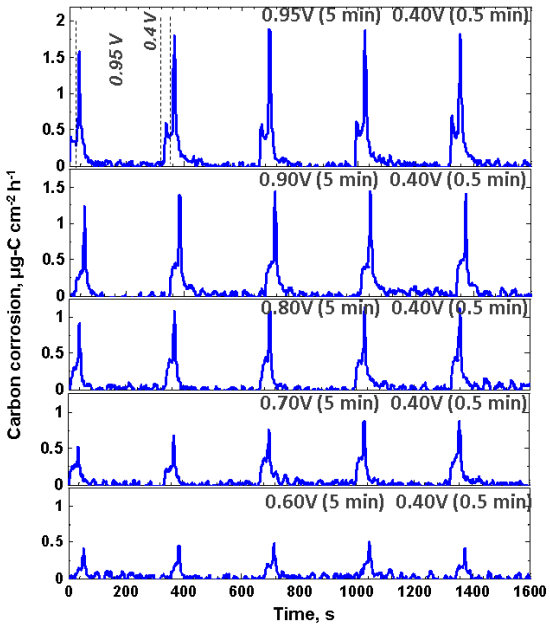

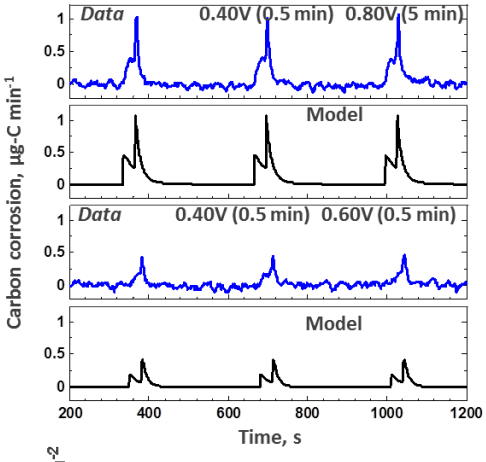

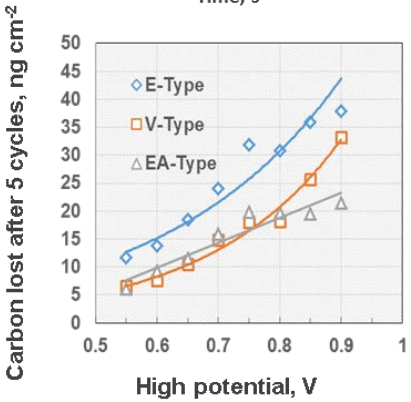

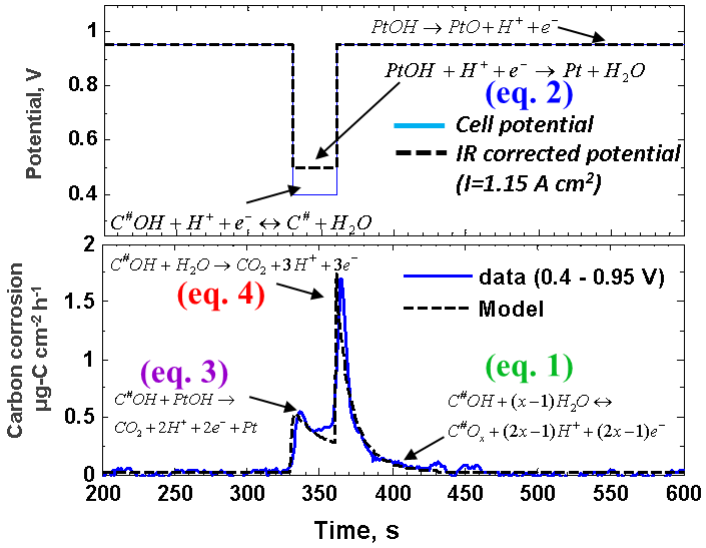

1) *Formation of active ($C^{\#}OH$) and passive ($C^{\#}O_x$) carbon surface oxide species*

2) *Formation of OH and oxide surface species on Pt*

3) *Oxidation of active carbon surface species ($C^{\#}OH$) with OH spill-over from Pt at intermediate potentials*

4) *Oxidation of active carbon surface species ($C^{\#}OH$) with H_2O at high potentials*

- For potential cycles to 0.8 V and higher (fixed 0.4 V low potential), corrosion rates are lower for graphitized carbon (EA-type) than for other carbons (E-type, V-type)
- For potential cycles below 0.8 V, the magnitude of corrosion upon a step change in potential is similar for all carbons
- Extents of corrosion linked to formation of carbon oxides and interaction of these oxides with Pt hydroxide and oxide and water

Accomplishment: Transient Corrosion Mechanism

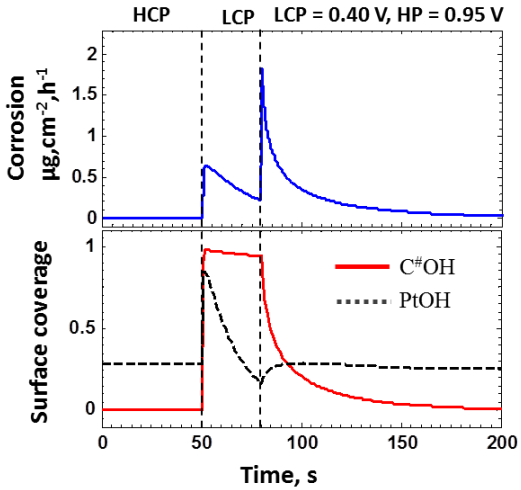

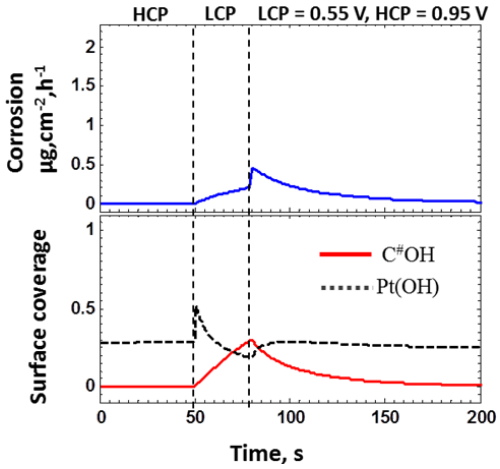

Varied Upper Potential Limit

0.95 V – 0.40 V
0.90 V – 0.40 V
0.85 V – 0.40 V
…..
0.55 V – 0.40 V

Varied Lower Potential Limit

0.95 V – 0.40 V
0.95 V – 0.45 V
0.95 V – 0.50 V
…..
0.95 V – 0.80 V

- **Low corrosion rate if cell held at high cell potential**
  - Defect sites passivated by $C^{\#}O_x$
  - Pt exists mainly as PtO at 0.95 V and as Pt at 0.6 V
- **Small corrosion spike in transitioning from HCP to LCP**
  - $C^{\#}O_x$ begins to convert to active $C^{\#}OH$
  - PtO converts to PtOH
  - Spikes due to reaction between $C^{\#}OH$ and PtOH
  - Increasing lower cell potential from 0.4 to 0.55 V decreases corrosion during transition due to lower equilibrium $C^{\#}OH$ coverage
- **Corrosion rate slowly decreases as the cell is held at low cell potential**
  - PtOH converts to Pt
- **Large corrosion spike in transitioning from LCP to HCP**
  - Spikes due to rapid reaction between $C^{\#}OH$ and H_2O at elevated potential
  - $C^{\#}OH$ converts to $C^{\#}O_x$ over longer time
  - PtOH converts to PtO over longer time

Accomplishment: Steady-State Corrosion Model

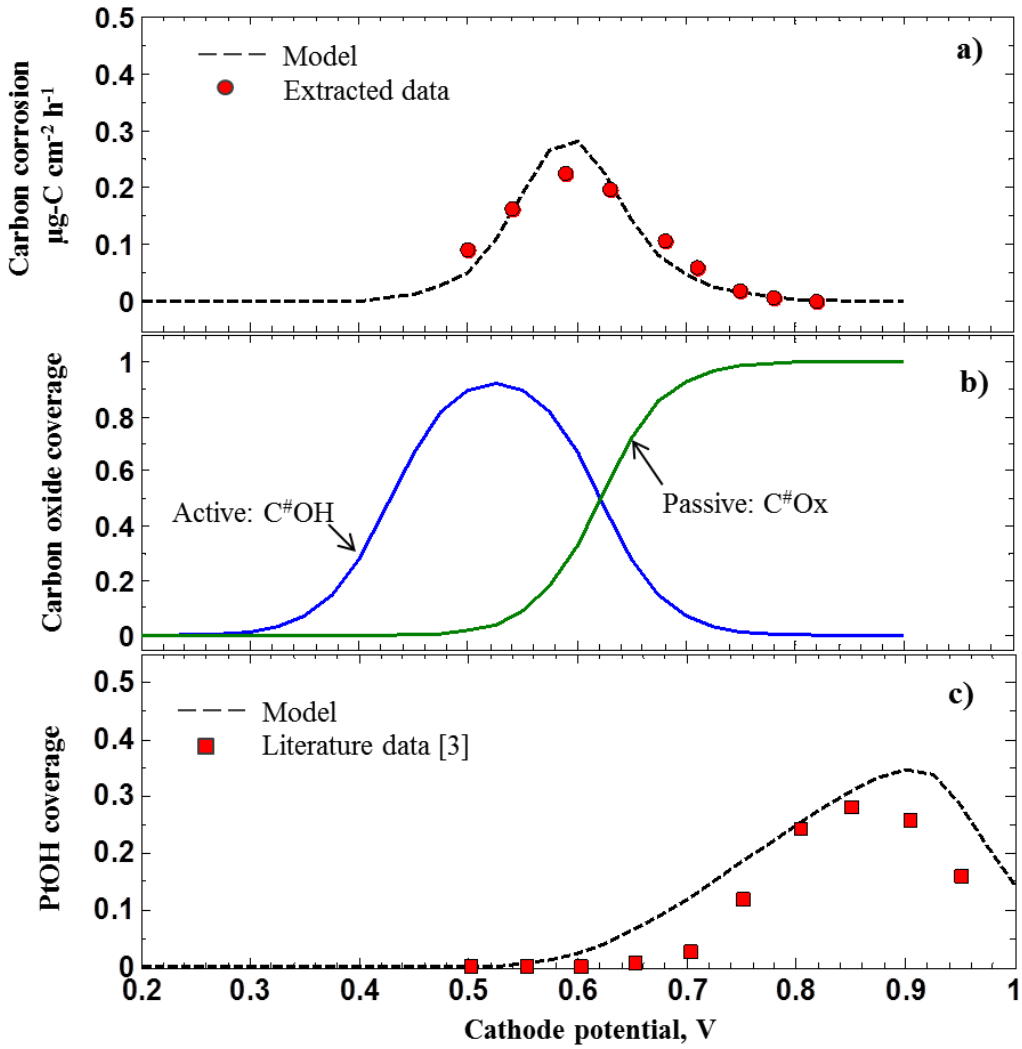

- Steady-state corrosion rates determined from NDIR data for CO_2 emission after 5-min hold at potential
- Over 0.4-0.95 V cathode potentials, steady-state corrosion rate peaks at ~0.6 V
- Peak corrosion rates are similar for E-Type, V-Type and EA-Type carbons

- Steady-state corrosion rate slows above 0.6 V due to formation of passive oxides

- Pt converts to PtOH above 0.6 V
- PtOH converts to PtO above 0.9 V
- **Since PtOH only forms above 0.6 V, the observed corrosion peaks are due to $C^{\#}OH$ reacting with H_2O.**

[3] Casalongue, H.S., et al. (2013). Nature Communications, 4, 2817.

Summary of Mechanism of Carbon Corrosion during Drive Cycles

- **Formation of surface oxides on carbon defect sites ($C^{\#}$)**
  - Defect sites hydrolyze to form active oxides ($C^{\#}OH$) at cathode potential (E) >0.3 V
  - $C^{\#}OH$ converts to passive oxides ($C^{\#}O_x$) at E >0.8 V
- **Carbon corrosion is catalyzed by PtOH**
  - PtOH begins to form at E >0.6 V
  - PtOH converts to PtO at E >0.9 V

1) Formation of active ($C^{\#}OH$) and passive ($C^{\#}O_x$) carbon surface oxide species

$$C^{\#} + H_2O \leftrightarrow C^{\#}OH + H^+ + e^-$$

$$C^{\#}OH + (x-1)H_2O \leftrightarrow C^{\#}O_x + (2x-1)H^+ + (2x-1)e^-$$

2) Formation of OH and oxide on Pt

$$Pt + H_2O \leftrightarrow PtOH + H^+ + e^-$$

$$PtOH \leftrightarrow PtO + H^+ + e^-$$

3) Oxidation of $C^{\#}OH$ with OH spill-over from Pt

$$C^{\#}OH + PtOH \rightarrow CO_2 + 2H^+ + 2e^- + Pt$$

4) Oxidation of $C^{\#}OH$ with H_2O

$$C^{\#}OH + H_2O \rightarrow CO_2 + 3H^+ + 3e^-$$

- **Steady-state corrosion mechanism**
  - Corrosion rate peaks at ~0.6 V cathode potential, small at 0.95 V
  - Corrosion is primarily due to oxidation of $C^{\#}OH$ by H_2O
  - All three carbons (Ketjenblack, Vulcan and graphitized Ketjenblack) show similar corrosion rates
- **Carbon corrosion under transient potentials can be much higher**
  - Spikes in corrosion rates while transitioning from high (0.95 V) to low cell potentials (0.4 V) are due to formation of $C^{\#}OH$ and its and its reaction with PtOH
  - Larger spikes in corrosion rates while transitioning from low (0.4 V) to high cell potentials (0.95 V) are due to accelerated oxidation of $C^{\#}OH$ by H_2O at elevated potentials
- **Transient corrosion rates: E-Type ~ V-Type >> EA-Type**

Proposed Near-term Future Work

- Potentiostatic and potential cycling dissolution and oxide coverage measurements for IRD Pt_3Co and Umicore Pt_3Co
  - Comparison of catalysts with “spongy” morphology to “solid” morphology
- Measurements of Pt re-deposition rates as a function of potential
- Application of catalyst corrosion model to cell data using TEM-EDAX and XRF quantification of Pt and Co in cell components
- EXAFS analysis of changes in Pt and Co coordination numbers and bond distances for catalysts from cycled MEAs
- Delta-μ XANES analysis of Pt_3Co oxide structure as a function of potential (in collaboration with General Motors)
- Solid state microelectrode measurements of oxygen permeability
  - Impact of Co^{2+} and Ni^{2+} as a function of relative humidity and temperature
- Carbon corrosion studies for Pt alloys vs. Pt of similar particle size distribution
- Pt dissolution as a function of carbon type and correlation with changes in particle size distribution and electrochemically-active surface area

Summary

- **Relevance:** Realize the ORR mass activity benefits of advanced Pt-based cathode electrocatalysts in high current density, air performance for over 5,000 operating hours and with low PGM loading ($\leq$0.1 mg-Pt/cm^2)
- **Approach:** Studies of catalyst and catalyst support durability and degradation mechanisms, catalyst/support interactions, and effects of catalyst instability on cathode-catalyst-layer properties
- **Accomplishments and Progress:** Determined potential and potential cycling dependence of Pt and Co dissolution from several Pt_3Co alloys, oxide formation kinetics and thermodynamics, and developed a model based on these data for the thermodynamics and kinetics of Pt and Co loss from catalyst particles; Initiated solid-state cell work for oxygen permeability measurements in ionomer thin films; Developed a model for carbon corrosion during drive cycle.
- **Future work:** Potentiostatic and potential cycling dissolution and oxide coverage measurements for IRD Pt_3Co and Umicore Pt_3Co and other advanced catalysts with alternative morphologies/properties; Measure Pt re-deposition rates; Apply catalyst corrosion model to MEA data; Determine changes in catalyst atomic composition and distribution using XANES; Solid-state measurements of effect of base metal on oxygen permeability; Refinement of cathode performance and durability model using *ex situ*-measured component properties.